Sci. J. Fac. Sci. Minufia Univ., 2008, Vol. XXII, 147 - 168

GEOLOGY, GEOCHEMISTRY AND RADIOACTIVITY OF DYKES AT GABAL MINADIER AREA, SOUTHCENTRAL SINAI, EGYPT

ALI ALI ABDEL RAHMAN EL MOWAFY
Nuclear Materials Authority, P. O. 530, Maadi, Cairo, Egypt.

ABSTRACT

Gabal Minadier area is dissected by dyke swarms composed of rhyolite, andesite and basaltic-andesite. The rhyolite dykes are the oldest and dominantly oriented NE with minor deviations of varieties their trends to NNE and ENE directions. They were related to a stress orientation plunging 65° to S50°E direction. The andesite dykes are oriented mainly to NW, which related to an extensive extensional tectonic in the NE-SW direction where the stress is plunging 80° in the S60°W direction. The basaltic-andesite dykes have mainly NNW, NW and NE trends. These dykes represent the terminate emplacement of the studied dykes. They were related to extensional event in NE-SW direction where the stress ellipsoid is plunging 60° in the S38°W direction. All of them originated from calc alkaline magma in arc lava and MORB. They have high enrichment in LIL (Ba and Sr) and show mildly enrichment in the HFSE (Nb and Zr). Uranium mineralization is lithologically and structurally controlled, as it is restricted to the NE trending rhyolite dykes. Pyrochlore, betafite, schoepite, euxenite, uranothorite and zircon are radioactive minerals recorded.

Key words: Ryolite,andesite,basaltic-andesite, dykes, G.Mindair, Sinai, Egypt.

INTRODUCTION

The marked planar of the interface between many of the intrusive dykes and their hosting granitic pluton is commonly interpreted as the result of their magma emplacement along joint-like fractures (Balk, 1937; Martin, 1952; Hutchinson, 1956). The Neoproterozoic cratonization of Sinai and Eastern Desert of Egypt were accompanied by extensive granite plutonism followed by several episodes of crustal extension and dykes emplacement. These dykes are chronologically classified as post granite dykes (El Ramly and Akaad, 1960) and are related to a regional extensional tectonics at the latest stages of Pan-African tectonic cycle (Stern et al., 1984; Stern and Hedge, 1985). Akaad and El Ramly (1960) and Stern and Hedge (1985) distinguished the dyke intrusions in Egypt into three main episodes: a) Late Precambrian metamorphosed dykes, b) Late

Precambrian unmetamorphosed dykes, and c) Neogene dykes. Stern and Hedge (1985) stated the dykes of the first episode were emplaced and metamorphosed under amphibolite and greenschist facies conditions. El Ramly and Akaad (1960) described the unmetamorphosed dykes as the "post granite dykes'', where they post-date the folding and metamorphic events of the Egyptian basement complex. Stern et al. (1984) mentioned the Neogene dykes are of basic composition and mostly pertain to the early rifting stages of the red sea.

The post- granite dykes represent the latest waning phases of magmatism during the pan-African orogeny. They cut through all the Precambrian rocks and consist of variable rocks ranging from basaltic to rhyolitic types, including several generations of subalkaline and alkaline series (El Ramly and Akaad 1960). The dyke swarms associated with rifting and sea-floor spreading commonly trend normal to the direction of maximum extension (Ross, 1983; Druecker, 1985; Goldberg and Buttler, 1985), whereas those associated with plate convergence, trend parallel to the direction of maximum compression (Ross, 1983; Feraud et al., 1985; Hooper and Subbarao, 1985).

Individual dykes, which are emplaced at intervals during the episodes of crustal thickening, may be used as indication of the orientations and changing of the horizontal stress field affecting the earth's crust with time during the dyke emplacement.

The present study deals with the geology, geochemistry and radioactivity of dykes at Gabal Minadier South Central Sinai. The study area covers about 90 km^2 and is situated between latitudes 28° 40` 32`` and 28° 45` 40`` N and between longitudes 33° 54` 12`` and 34° 03` 48`` E (Fig. 1).

FIELD RELATIONS AND STRUCTURAL SETTING

Several studies on dyke rocks in Sinai are carried out, e.g. Feraud et al. (1985), Eyal and Eyal (1987), Zalata (1988), Friz-Töpfer (1991), Mousa (1994) and Katta (1994). They dealt in detail with the petrography, geochemistry, relative ages and regional trends of these dykes. Most of these studies deal with the calc-alkaline dykes, while few of them gave attention to the alkaline dykes. The geology of Gabal Minadier area has been studied by El Metwally (1997). The area comprises older granites composed of quartz-diorite, tonalite and granodiorite, younger gabbros and younger granites composed of alkali-granite. These rock units are highly invaded by dyke swarms (Fig.2).

The investigated dykes comprised rhyolite, andesite and basaltic-andesite varieties. They form prominent ridges cutting all rock units in the studied area. They were intruded at different periods as the rhyolite dykes are cut by andesite dykes and both of them invaded by the basaltic- andesite. The rhyolite dykes are

more resistant to weathering than the granitic host rocks whereas the andesite and andesitic-basalt dykes are less resistant to weathering. According to the field relations the rhyolite dykes are the oldest one then followed by andesite and basaltic-andesite dyke swarms. Generally, the basaltic-andesite dykes are the youngest. These entire dyke swarms posses sharp contacts with their host rocks and they are commonly steeply inclined (65°-80°).

The rhyolite dykes are the dominant constituting about 60% of the studied dykes. They are dominantly oriented to the NE except some minor deviation to the NNE and ENE directions (Fig.3.a). They usually range from 2 m to 10 m in thickness and from 1.5 km to 9 km in length. They form positive relief relative to their host and usually show a pronounced grain size increasing from their margins to the center. The paleostress analysis of the rhyolite dyke trends reveal that they were related to a stress ellipsoid orientation with σ_3 plunging 65° in S50°E direction, σ_2 plunges 60° in S45°W direction and σ_1 plunging 40° in N15E direction (Fig.4a).

The andesite dykes constitute about 15% of the studied dykes. They intrude all the basement rocks of the studied area and trend mainly in the NW direction (Fig.3c). This structural trend is related to the extensive extensional tectonics in the NE-SW direction where σ_3 plunging 80° in the S60°W direction, σ_2 plunges 65° in the S35°E direction and σ_1 plunging 30° in the N25W direction (Fig.4c).

They represent the terminate emplacement of the dyke intrusions at Gabal Minadier area. They range usually from 1.5 m to 8 m in thickness and from 1.1 km to 7.5 km in length. They intrude all the basement rock units of the studied area and trend mainly NNW, NW and NE (Fig.3b). These trends are related to the extensional event in the NE-SW direction where the stress ellipsoid is oriented with σ_3 plunging 60° in the S38°W direction, σ_2 plunges 70° in the S55°E direction and σ_1 plunging 40° in the N30° E direction (Fig.4b).

Generally, the paleostress analyses of the studied dyke trends indicate that the rhyolite dykes are related to an extensive extensional tectonic where the axis of maximum extension plunges 65° in S50°E direction. The andesite and basaltic-andesite dykes have axes of maximum extension plunges 80° and 60° in S60W and S38°W respectively. Summary of the dyke trends and paleostress analyses are shown in Table 1.

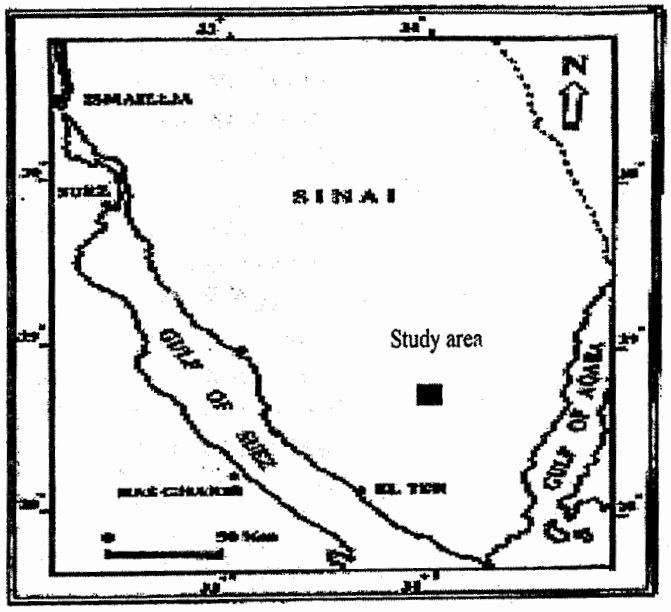

Fig. (1): Location map of the studied area

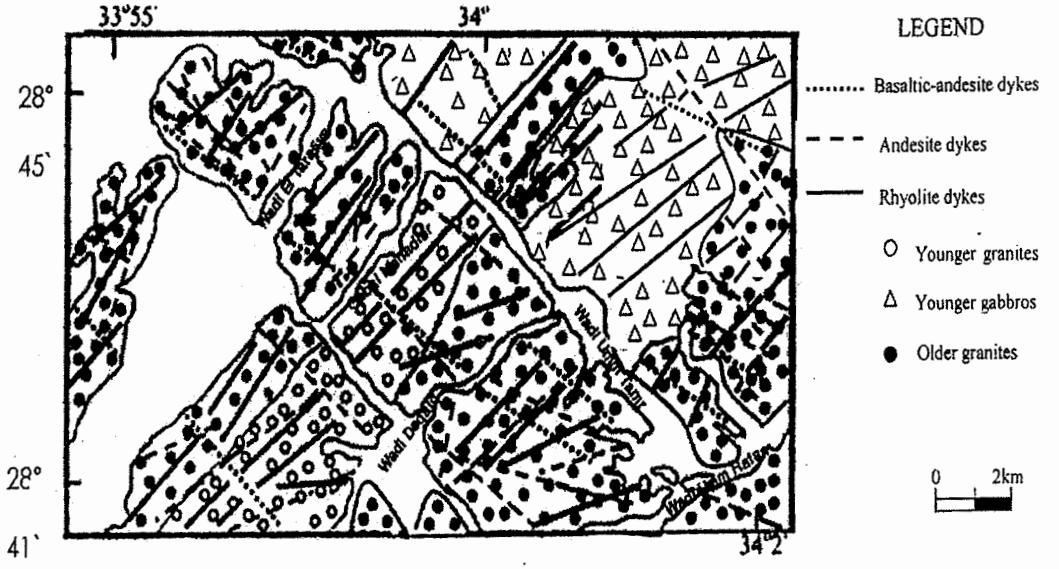

Fig. (2): Geological Map of Gabal Minadier Area (Modified after El Metwally, 1997)

Table 1: Summary of the dyke trends and paleostress analyses

Dykes	Trend	σ1	σ2	σ3
Rhyolite dykes	NE> ENE>NNE	15 / 40	225/ 60	130 / 65
Andesite dykes	NW	335 / 30	145 / 65	240 / 80
Basaltic-andesite dykes	NNW>NW>NE	30/ 40	125 / 70	218 / 60

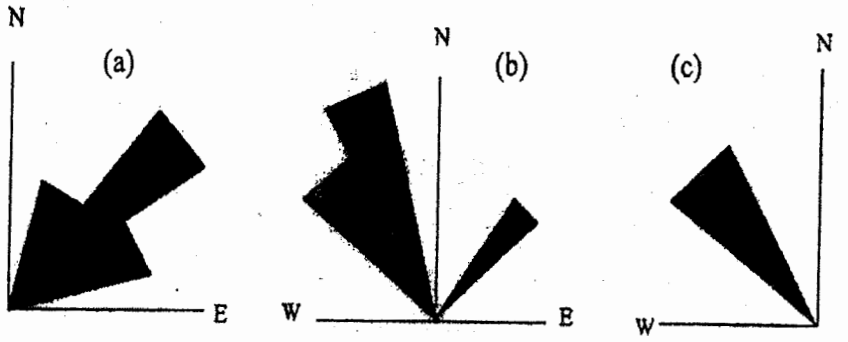

Fig. (3): Rose diagram of different dyke trends at Gabal Minadier area.

(a): Rhyolite dykes (b): Basaltic-andesite (c): Andesite dykes

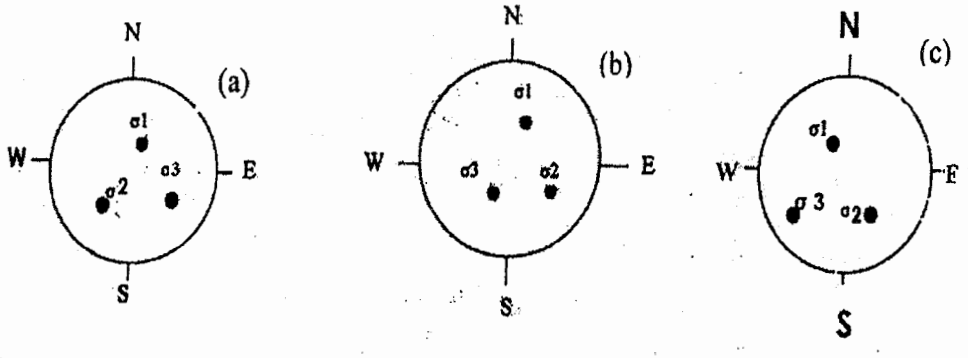

Fig. (4): Orientation of stress ellipsoid intrusion of studied dykes at Gabal Minadier area.
(a): Rhyolite dykes (b): Basaltic-andesite dykes (c): Andesite dykes

PETTROGRAPHY

Rhyolite dykes

Rhyolite dykes are composed of K-feldspar, quartz and plagioclase (An4-18) phenocrysts embedded in a fine-grained quartzo-feldspathic groundmass. Accessory minerals include allanite, apatite, zircon and opaques. K-feldspar is mainly sanidine, which moderately altered to sericite at the crystal core. Quartz is present as subhedral crystals and exhibits undulatory extinction. Plagioclase (An4-18) occurs as prismatic and tabular crystals. Granophyric, spherulitic and porphyritic textures are encountered. Granophyric and spherulitic textures intergrowth is developed at the peripheries of phenocrysts due to reaction with matrix. The spherulitic pattern consists of radially disposed fibrous crystals of intergrown quartz and alkali feldspar, while micro-graphic intergrowth usually fill the interstices and form a granophyric rims around the present phenocrysts (Fig.5).

Andesite dykes

They are either aphyric or porphyritic rocks with about 15% phenocrysts that reach up to 3.0 mm x 1.2 mm in size. They are mainly composed of plagioclase (An_{35-45}), brown hornblende, reddish brown biotite, quartz and augite. Epidote, apatite and opaques are the accessory minerals. These constitute embedded in a fine-grained matrix of the same composition. Amygdales are well developed and filled with quartz and hornblende (Fig.6). Plagioclase is usually replaced by saussurite. They showing faint albite and combined Carlsbad-albite twinning. Hornblende is occasionally twinned and shows corroded margins due to variable degrees of alteration to chlorite. Biotite is frequently replaced by chlorite, and opaque mineral granules along their peripheries and cleavage planes. Augite is strongly pleochroic with dark to yellowish green colour.

Basaltic-andesite dykes

They are composed essentially of phenocrysts of plagioclase, augite and hornblende set in a fine-grained groundmass consisting of plagioclase, augite and brownish red hornblende. Accessory minerals are sphene, apatite and opaques. Plagioclase (An_{40-58}) is mainly andesine to labrodorite, occurring as subhedral crystals commonly twinned (Fig. 7) and zoned with marked epidote and zoisite aggregates. Augite is present as subhedral prismatic crystals and moderately altered to actinolite and/or chlorite. Hornblende usually forms euhedral brownish red crystals with perfect six-sided outlines (Fig.8).

epidote and zoisite aggregates. Augite is present as subhedral prismatic crystals and moderately altered to actinolite and/or chlorite. Hornblende usually forms euhedral brownish red crystals with perfect six-sided outlines (Fig.8).

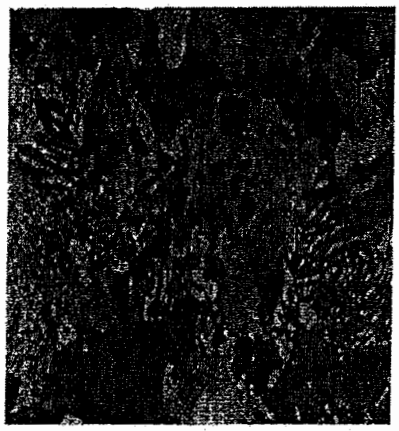

Fig. (5): Granophyric texture in rhyolite dykes

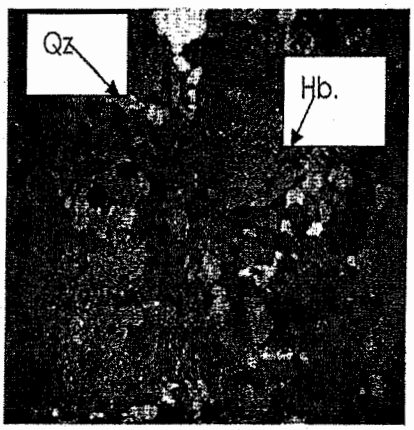

Fig. (6): Amygdales filled with quartz (Qz) and hornblende (Hb)

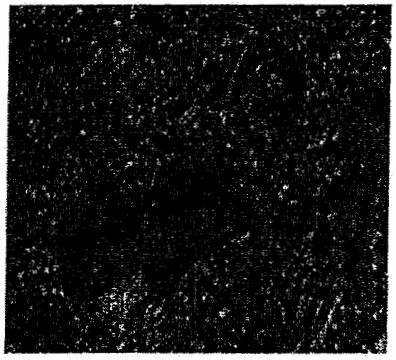

Fig. (7): Plagioclase (Plg.) phenocrysts embedded fine grained ground mass in basaltic-andesite

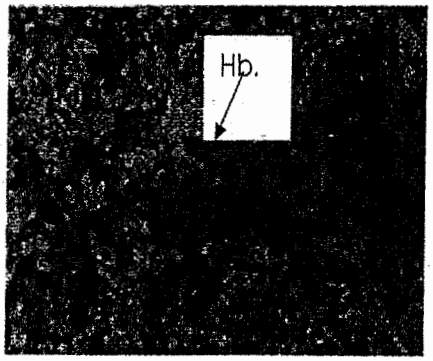

Fig. (8): Brownish red hornblende (Hb.) crystal in in basaltic- andesite dykes

GEOCHEMISTRY

Analytical techniques

The chemical analyses of twenty-eight dyke samples for major oxides and some trace elements were carried out using a PW 1404 XRF spectrometer following the procedures of Philips (1994) for correction of matrix. These instruments are hosted in mineralogical Institute, Trieste University, Italy. Major and trace element analyses of different studied dykes in Gabal Minadier area are shown in Table 2.

Geochemical classification

The classification of the studied dykes was geochemically confirmed by plotting the analyses on the $Na_2O + K_2O$ versus SiO_2 diagram (Fig.9) suggested by Le Bass et al. (1986). It shows that the analyzed samples fall in the fields of basaltic-andesite, andesite and rhyolite.

Chemical characteristics

Chemical variations within rocks of one or more magma series of different regions may be visualized by applying Harker diagrams. The major element variations relative to SiO_2 are used as an index of differentiation for the studied dykes (Fig.10). The oxides Al_2O_3, CaO, FeO^t, and MgO decrease regularly from basaltic-andesite and andesite to rhyolite with increasing SiO_2. On contrast, K_2O and Na_2O show a continuous increase with increasing SiO_2. The curved linear systematic variations for most of the major oxides in the studied dykes could be interpreted as evidence of fractional crystallization.

Magma types

Al_2O_3/TiO_2 versus TiO_2 diagram (Fig.11) after Sun and Nesbit (1978) shows that the studied dyke samples fall along the same trend. This suggest that they result from continuity of magmatism with high TiO_2 magma being the least fractionated (basaltic-andesite), while the lower TiO_2 magma represented the more fractionated varieties (rhyolite). In the FAM diagram (Fig.12), the studied dyke samples fall clearly within the calc-alkaline field.

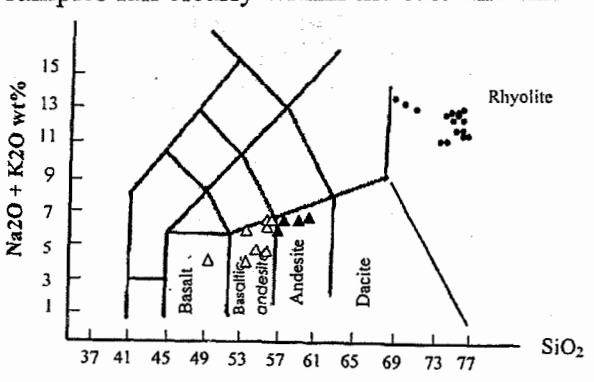

Fig. (9): SiO2 versus total alkalis diagram after Le Bass et al. (1986), showing the fields occupied by the studied dykes

Sample symbols
Rhyolite ●
Andesite ▲
Basaltic-andesite △

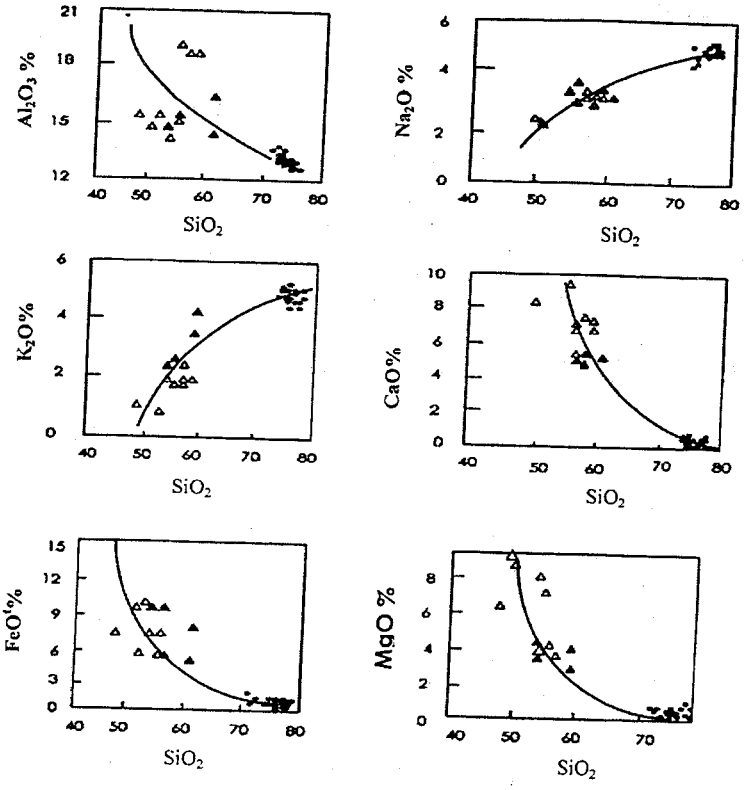

Fig. (10): Harker variation diagram for the different studied dykes. Symbols as in Fig. 9

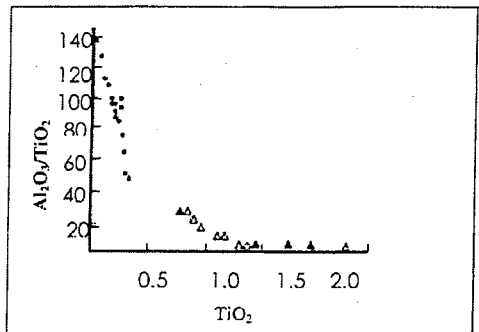

Fig. (11): Al_2O_3/TiO_2 versus TiO_2 binary diagram of studied dykes (after Sun and Nesbit, 1978). Symbols as in Fig. 9

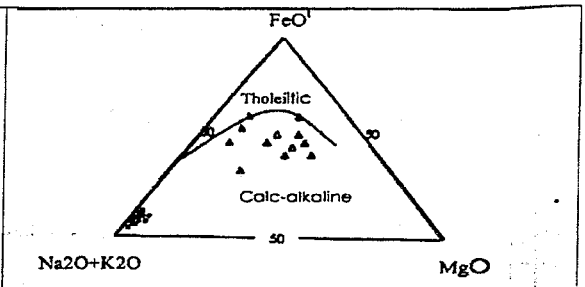

Fig. (12): AFM diagram of the studied dykes in Wadi Minadier area. The boundary between tholeiitic and calc-alkaline rocks is taken from Irvin and Baragar (1971). Symbols as in Fig. 9

Tectonic implication

Pearce and Cann (1973) used the Zr and Ti contents of volcanic rocks from known tectonic environment to develop tectonic discrimination diagram suitable to identify the tectonic setting of volcanic rocks and discriminate between

mid-oceanic ridge basalt, arc lava and within-plate lava. The studied dyke samples were plotted on this diagram (Fig. 13). It shows that, the rhyolite samples plot in the arc lava field whereas the andesite and basaltic-andesite plot in both arc lava and mid oceanic ridge basalt.

From the Na_2O / K_2O versus Na_2O + K_2O diagram (Fig. 14) which was proposed by Miyashiro (1975), the plots are clustered either in or close to the field of Eastern Asia continental alkali rocks and Atlantic island alkaline rocks and within the field of island-arc volcanic rocks. Two trends in the evolution of modern volcanic rocks in eastern Asia (Chengzao, 1987) are illustrated on this diagram. The first is form island arc andesites to alkaline rocks, implying that the tectonic setting changes from island arc to back arc. The second ranges from island arc andesites to rhyolites, implying that the tectonic setting changes from immature to a mature island arc or active continental margin.

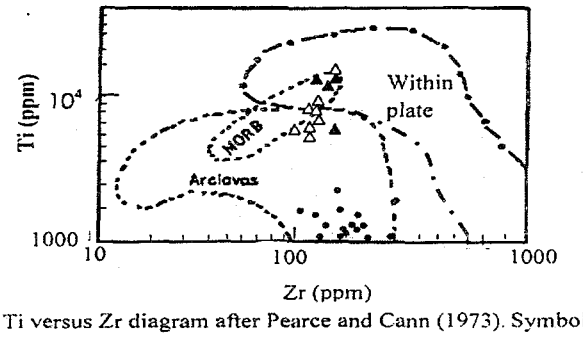

Fig.(13): Ti versus Zr diagram after Pearce and Cann (1973). Symbols as in Fig. 9

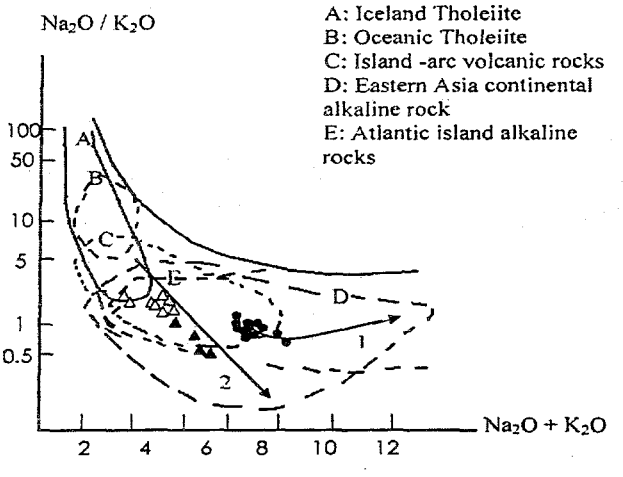

Fig. (14): Na_2O / K_2O versus Na_2O + K_2O diagram after Miyashiro (1975). Symbols as in Fig. (9)

Incompatible trace element pattern

The average incompatible element contents for the studied dykes are normalized to MORB values of Pearce (1983) and are illustrated in figure 15. The normalized multi-element spiderdiagram of the rhyolite, basaltic-andesite and andesite dykes show high enrichment in Ba and Sr, mild enrichment in Nb, Zr, Ce and La. The K is slightly enriched in rhyolite and andesite than andesitic-basalt. On other hand, they show high depletion in Rb, Nd and Y. The high enrichment in LIL (Ba and Sr) may reflect the studied dykes are related to subducted oceanic slab in their parent magma at destructive plate margins (Tatsumi et al., 1986; Wyllie et al., 1989). The
mildly enrichment in the HFSE (Nb and Zr) in the studied dykes indicates the involvement of mildly enriched sub-continental lithospheric mantle in their magma source (Pearce, 1983).

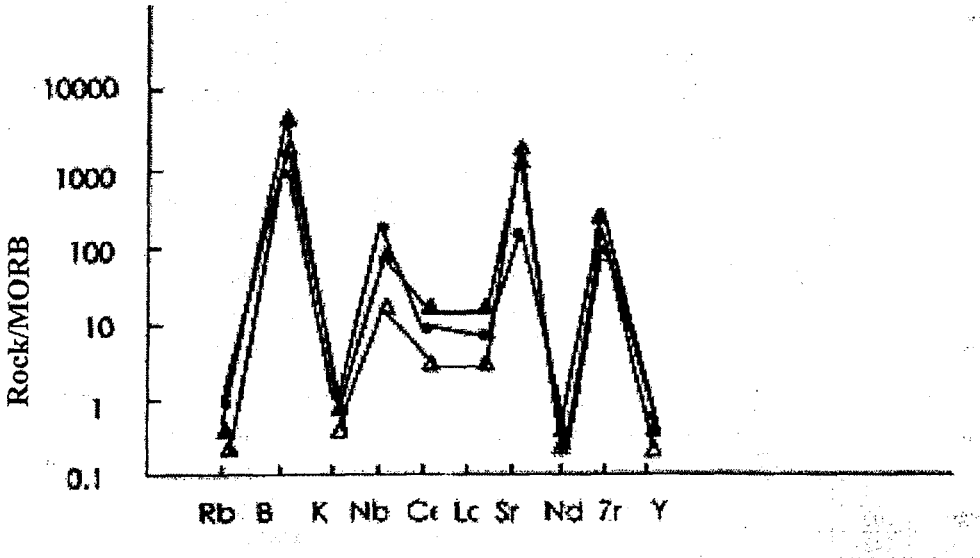

Fig.15: MORB normalized multielement plots of different studied dykes. Normalized values are from Pearce (1984). Symbols as in Fig. 9

Table 2: Major oxides (wt%) and trace elements (ppm) of the studied dykes

Rocks	Rhyolite													
Sample	1	2	3	4	5	6	7	8	9	10	11	12	13	14
SiO_2	76.23	76.34	76.56	76.01	75.98	76.01	76.20	76.02	73.03	74.16	72.36	76.41	76.75	76.54
Tio_2	0.14	0.15	0.16	0.15	0.18	0.17	0.19	0.18	0.30	0.23	0.34	0.16	0.17	0.15
Al_2O_3	13.16	13.11	13.15	13.11	13.19	13.29	13.91	13.41	14.20	14.20	14.71	12.79	12.64	13.11
FeOt	1.32	1.43	0.95	1.03	0.97	0.94	0.88	0.83	1.31	0.99	1.38	1.59	1.10	0.84
MnO	0.03	0.03	0.06	0.05	0.05	0.04	0.04	0.24	0.04	0.05	0.08	0.01	0.11	0.08
MgO	0.01	0.09	0.04	0.08	0.05	0.00	0.08	0.08	0.38	0.20	0.49	0.07	0.06	0.03
CaO	0.03	0.01	0.14	0.37	0.24	0.40	0.13	0.07	0.70	0.46	0.53	0.02	0.41	0.25
Na_2O	5.30	5.27	4.69	4.71	4.67	4.80	4.96	4.57	4.65	4.97	4.38	4.55	4.58	4.75
K_2O	3.78	3.56	4.24	4.48	4.66	4.34	4.62	4.60	5.32	4.72	5.67	4.39	4.18	4.25
P_2O_5	0.00	0.01	0.01	0.01	0.01	0.01	0.01	0.00	0.07	0.02	0.06	0.01	0.00	0.00
L.O.I.	0.00	0.00	0.00	0.00	0.00	0.00	0.00	0.00	0.00	0.00	0.00	0.00	0.00	0.00
Total	100	100	100	100	100	100	100	100	100	100	100	100	100	100
Cr	0	0	0	0	0	0	0	0	0	0	0	0	0	0
Ni	4	5	7	4	6	5	3	4	4	4	7	6	6	3
Ba	20	201	61	10	26	15	86	154	722	154	912	118	7	12
Rb	138	102	140	195	173	168	158	182	172	158	168	210	192	202
Sr	28	70	35	54	42	42	27	25	104	31	91	31	23	12
La	25	26	46	48	45	50	85	57	72	76	76	49	34	34
Ce	93	102	94	101	96	102	139	97	130	148	138	105	84	77
Nd	25	30	37	38	36	39	67	42	58	68	71	49	48	42
Zr	246	296	236	196	195	200	209	185	214	230	311	144	230	130
Y	59	70	59	50	49	50	51	50	38	48	50	44	76	65
Nb	39	37	39	36	35	37	32	35	21	29	27	43	42	34

Table 2: (Cont.)

Rocks			Andesite				Basaltic - andesite							
Sample	15	16	17	18	19	20	21	22	23	24	25	26	27	28
SiO_2	75.42	75.54	60.44	56.89	56.27	60.25	56.51	53.57	55.72	56.67	57.38	56.78	53.62	49.31
Tio_2	0.17	0.18	0.79	1.96	1.71	1.44	1.18	0.91	0.88	0.90	0.94	1.03	1.32	2.20
Al_2O_3	13.71	13.45	16.59	14.95	14.82	14.26	14.47	15.15	19.14	18.15	18.77	13.91	14.32	15.21
FeOt	0.89	1.15	5.40	10.72	10.72	8.06	8.39	9.74	6.34	6.77	6.37	8.39	9.55	13.54
MnO	0.05	0.03	0.14	0.16	0.15	0.19	0.12	0.16	0.10	0.11	0.10	0.13	0.16	0.18
MgO	0.09	0.06	3.67	3.09	4.04	2.50	7.01	9.12	3.72	4.19	3.36	8.11	8.36	6.56
CaO	0.57	0.48	5.24	5.19	5.66	4.96	7.03	7.88	9.19	8.31	7.78	5.94	7.07	8.54
Na_2O	4.30	4.23	3.28	3.70	3.69	3.37	3.38	2.39	3.06	3.06	3.55	3.24	3.09	2.66
K_2O	4.78	4.86	4.19	2.74	2.26	3.59	1.56	0.84	1.58	1.57	1.46	2.13	1.99	1.19
P_2O_5	0.02	0.02	0.26	0.59	0.68	1.38	0.35	0.24	0.27	0.27	0.29	0.34	0.52	0.80
L.O.I.	0.00	0.00	0.00	0.00	0.00	0.00	0.00	0.00	0.00	0.00	0.00	0.00	0.00	0.00
Total	100	100	100	99.99	100	100	100	100	100	100	100	100	100	99.99
Cr	0	0	20	10	15	2	322	323	35	41	21	365	272	84
Ni	7	3	21	7	7	10	101	84	28	27	26	124	100	50
Ba	146	200	1033	643	524	1451	961	355	350	388	394	620	571	363
Rb	160	142	91	87	66	68	40	37	47	48	41	67	49	34
Sr	45	54	435	509	495	619	917	501	702	636	675	723	795	595
La	50	38	47	33	30	84	25	20	17	19	16	26	23	25
Ce	106	75	86	75	76	201	66	51	41	52	50	66	60	66
Nd	53	33	45	47	49	108	33	28	22	21	25	30	35	47
Zr	181	104	211	227	225	235	152	123	123	121	134	137	154	20
Y	46	24	30	32	29	34	22	29	24	25	26	22	27	2
Nb	31	12	17	15	16	14	10	8	6	7	8	8	8	2

RADIOACTIVITY

Field radiometric survey was carried out using a calibrated portable gamma ray spectrometer, model Gs-256 (made in Czech), with NaI"Tl- detector, 75X75 mm^2. The uranium and thorium contents of the studied dykes were measured along dyke bodies. The spectrometric data reveals that there is a gradual increase in the eU and eTh contents from basaltic-andesite to andesite and reach the maximum values in rhyolite dykes (Table 2). Therefore, the rhyolite dykes are the most rock types recommended for uranium and thorium mineralization in the study area.

The eU-contents in the basaltic-andesite and andesite dykes have range between 1 to 3 ppm and the eTh contents range between 5 to 18 ppm. This indicates homogeneity in the distribution of both eU and eTh due to the narrow range of their distribution. The rhyolite dykes display the higher eU- and eTh-contents. The eU-contents range between 145 to 275 ppm and the eTh- contents range between 75 to 112 ppm (Table 3). The high values of eU/eTh ratios (av=2.12) and low values of eTh/eU ratios (av= 0.47) in the rhyolite dykes indicates high contents of uranium relative to thorium (Table 2). This may be attributed to the post magmatic addition of uranium.

The relationship between eU and eTh in the studied dykes indicates that the eU increases with increasing eTh from basic to acidic dykes (Fig. 16 a). On the other hand, the eU content decreases with increasing of the eTh/eU ratios from the acidic to basic dykes (Fig. 16.b). This confirms the post magmatic enrichment of uranium.

The relationship between the eU and both of Zr and Rb show positive relations (Figs 16 c & d respectively). This reflects the role of magmatic process in the uranium enrichment. However, Krauskopf (1979) stated that the Rb, Y, U and Th ions have large radii and are less extensive to substituting for major ions in common silicate minerals so they segregated and concentrated in late stages of melt differentiation.

Normally, Th is three times as abundant as U in the crust (Rogers and Adams, 1969). When eTh/eU ratio is disturbed, it indicates addition or removal of uranium because thorium is relatively stable during post magmatic processes. Pagel (1982) stated the decrease of Th/U is attributed to a slight decrease of the Th and increase of U contents at the end of the differentiation. The studied basic dykes show eTh/eU ratios ranging between 5.0 and 8.0 suggesting uranium leaching, whereas the acidic dykes have ratios ranging from 0,38 to 0.58 suggesting uranium addition during post magmatic processes. It could be

concluded that the radioactivity of the studied rhyolite dykes is related to magmatic and post-magmatic processes.

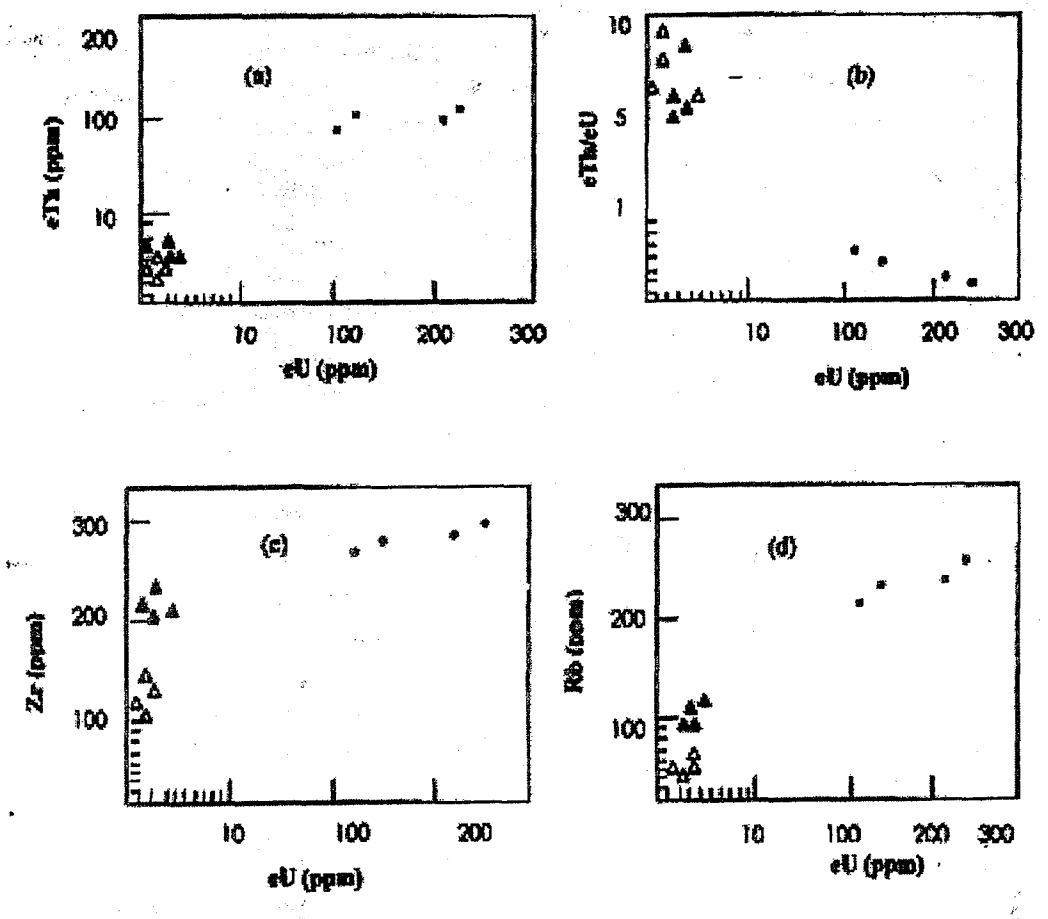

Fig.(16): eU variation diagrams (a) eU-eTh (b) eU-eTh/eU (c) eU-Zr (d) eU-Rb

The high radioactive samples were subjected to heavy liquid separation and XRD analysis for identification of the radioactive mineral(s). The identified minerals were confirmed by the EDX-SEM technique (Scanning Electron Microscope). These studies revealed the presence of pyrochlore, betafite, schoepite, euxenite, uranothorite and zircon in the studied rhyolite dykes. Betafite and euxenite are black in colour; uranothorite is yellow colour and they are visible by naked eyes as interstitial filling (Fig.17). Zone of zircon is petrographically recorded (Fig.18). The X-ray diffraction data are shown in (Fig. 19). Several spots

were analyzed by SEM technique along zones in betafite, exuenite and uranothorite grains and the back-scattered electron images are shown in (Figs.20, 21 and 22 respectively).

Pyrochlore $(Na,Ca)_2Nb_2O_6(OH,F)$ is a solid solution between the niobium end member (pyrochlore), and the tantalum end member (microlite). The mineral is associated with the metasomatic end stages of magmatic intrusions. Pyrochlore crystals are usually well formed (Euhedral), occurring usually as octahedra of a yellowish or brownish color and resinous luster. It is commonly metamict due to radiation damage from included radioactive elements.

Betafite $(Ca, U)_2 (Ti, Nb)_{2-6} (OH)$ is a popular uranium bearing mineral to collect. It is one of the few uranium minerals to form nice well shaped crystals. Because betafite has rare earth elements in its chemistry, it is one of several so called Rare Earth Oxides. Other rare earth oxides such as fergusonite, euxenite, aeschynite and samarskite have very similar properties to each other but lack betafite's typically well formed isometric crystals

Schoepite $(UO_2)_4O (OH)_6 \cdot 6H_2O)$ is a rare alteration product of uraninite in hydrothermal uranium deposits. It also may form directly from ianthinite.

Euxenite $(Y, Ca, Ce, U, Th) (Nb, Ta, Ti)_2O_6$ is a brownish black mineral with a metallic luster. It contains calcium, niobium, tantalum, cerium, titanium, yttrium, and typically uranium and thorium, with some other metals.

Uranothorite (Th, U) SiO4 is yellow to yellowish brown in colour. It is like thorite but contain uranium more than 10%.

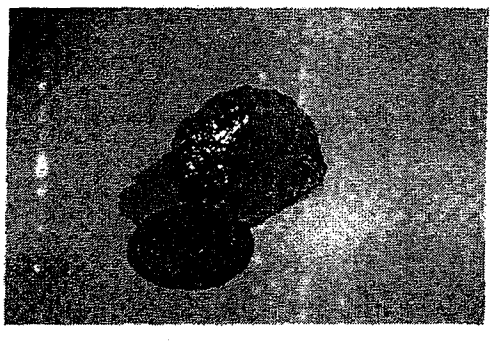

Fig. (17): Visible betafite, euxenite (black) and Uranothorite (yellow) minerals as interstitial filling.

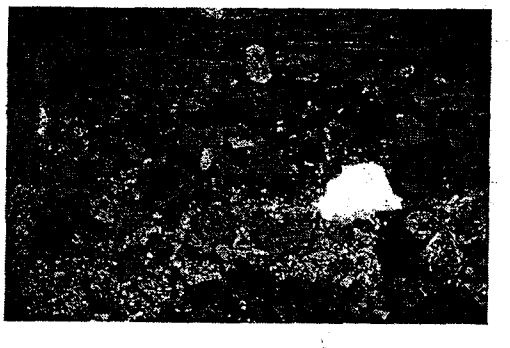

Fig. (18): Zone of zircon in studied rhyolite dykes

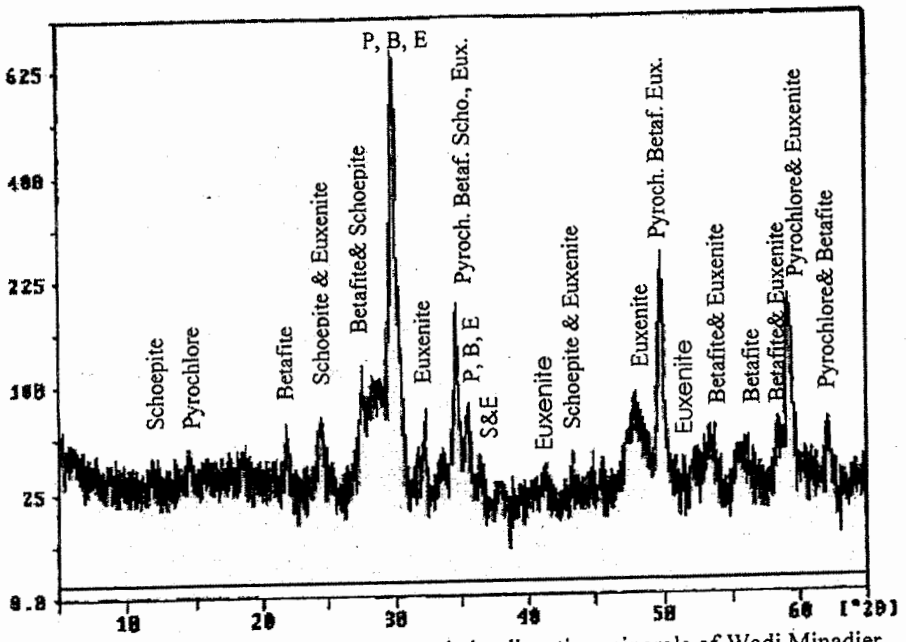

Fig. (19): X-Ray diffraction patterns of the recorded radioactive minerals of Wadi Minadier area.

Table 3: Results of Gamma ray spectrometric measurements of the studied dykes

Rock type	Serial N o.	eU (ppm)	eTh (ppm)	K%	eU/eTh	eTh/eU
Rhyolite	1	145	077	6.0	1.80	0.53
	2	270	112	9.0	2.40	0.41
	3	250	095	8.0	2.60	0.38
	4	130	075	5.0	1.70	0.58
Average		198.75	89.75	7.0	2.12	0.47
Andesite	5	1.0	5.0	2.5	0.20	5.0
	6	2.0	11	1.8	0.33	5.5
	7	2.0	14	2.0	0.50	7.0
	8	3.0	18	2.2	0.60	6.0
Average		2.0	12	2.12	0.40	5.9
Basaltic - andesite	9	1.0	6.0	1.6	0.33	6.00
	10	2.0	15	1.8	0.50	7.50
	11	1.0	8.0	1.5	0.25	8.00
	12	2.0	12	1.6	0.50	6.00
Average		1.5	10.25	1.62	0.40	6.87

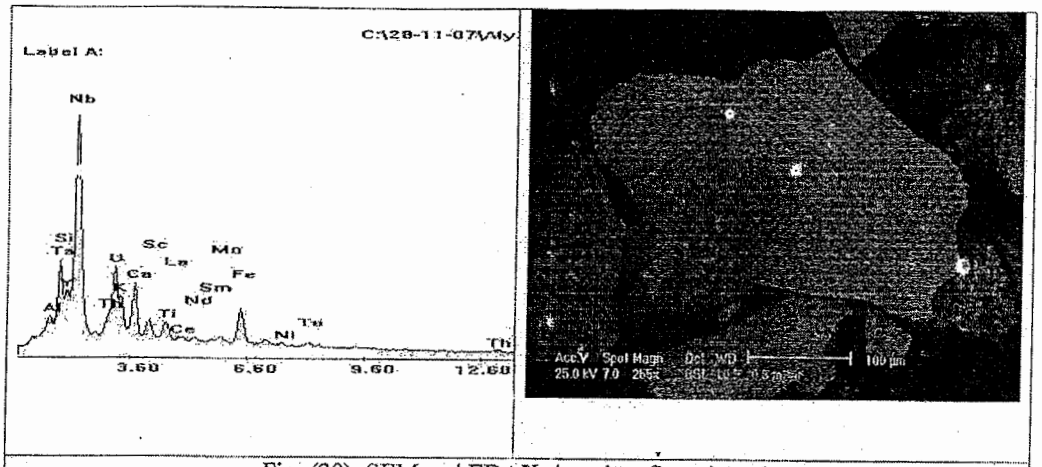

Fig. (20): SEM and EDAX show betafite mineral

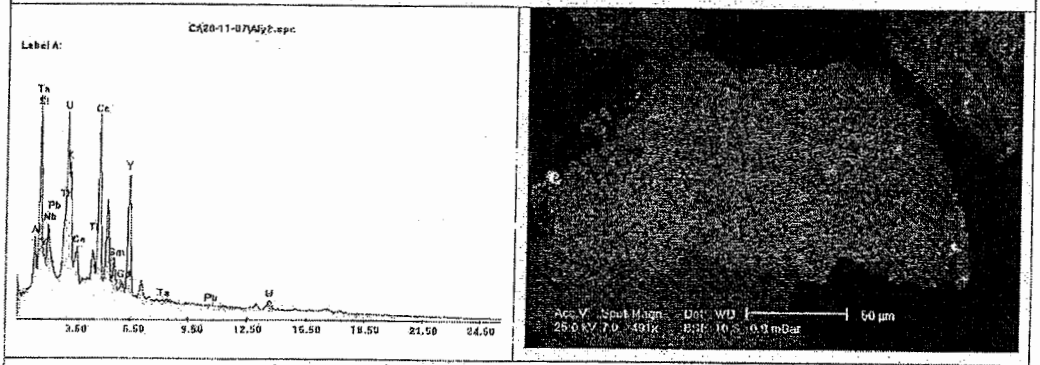

Fig. (21): SEM and EDAX show euxenite mineral

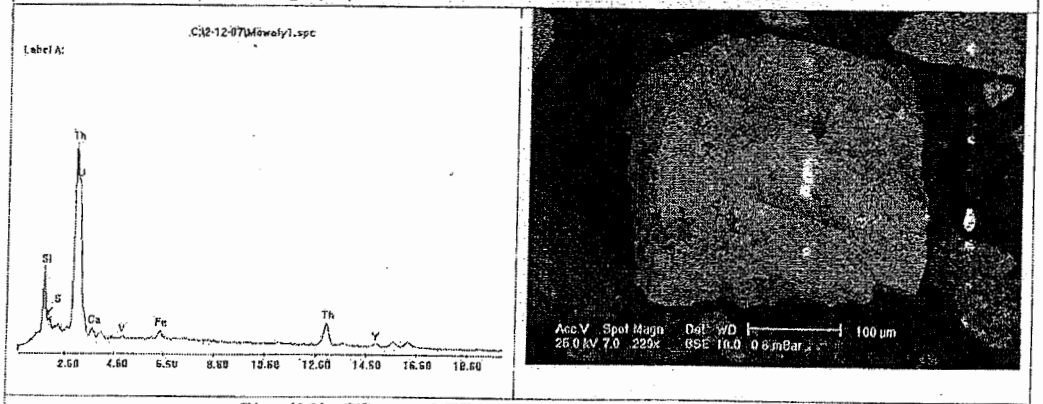

Fig. (22): SEM and EDAX show uranothorite mineral

CONCLUSIONS

The studied dyke swarms are composed of rhyolite, andesite and andesitic-basalt. The rhyolite dykes are dominant set and dominantly oriented in NE with some minor deviation of dyke trends by NNE and ENE. The paleostress analysis reveals that they were related to a stress ellipsoid orientation with σ_3 plunging 65° in S50°E direction, σ_2 plunges 60° in S45°W direction and σ_1 plunging 40° in N15E direction.

The andesite dykes represent the terminate emplacement of the dyke intrusion at Gabal Minadier area. They trend mainly NW which related to extensive extensional tectonics in NE-SW direction where σ_3 plunging 80° in S60°W direction, σ_2 plunges 65° in S35°E direction and σ_1 plunging 30° in N25Wdirection.

The basaltic-andesite dykes intrude all the basement rock units of the studied area and trend mainly NNW, NW and NE. These trends are related to extensional event in NE-SW direction where the stress ellipsoid is oriented with σ_3 plunging 60° in S38°W direction, σ_2 plunges 70° in S55°E direction and σ_1 plunging 40° in N30° E direction.

The studied dykes were derived from calc-alkaline magma, arc lava and MORB. They are enriched in LIL (Ba and Sr) reflecting the subducted oceanic slab in their parent magma at destructive plate margins. On other hand, they show mild enrichment in the HFSE (Nb and Zr) indicating the involvement of mild enriched sub-continental lithospheric mantle in their magma source.

The field radiometric survey and laboratory radiometric measurements indicated that the rhyolite dykes are the most important ones from the radioactivity point of view. This reflects the lithologic control of radioactivity. The NE rhyolite dykes are characterized by uranium and thorium mineralization. Consequently, the radioactive mineralizations are lithologically and structurally controlled. Pyrochlore, betafite, schoepite, euxenite, uranothorite and zircon are the main radioactive minerals in the examined dykes.

REFERENCES

Akaad, M.K. and El Ramly, M.F., 1960, Geological history and classification of the basement rocks of the Central Eastern Desert of Egypt. Geol. Surv. Egypt, paper, 9, 24 pp.

Balk, R., 1937, Structural behavior of igneous rocks. Geol. Soc. Am. Mem., S: 177pp.

Chengzao, J: 1987, Geochemistry and tectonics of the xionger group in the eastern qinling Mountains of China- a mid Proterozoic volcanic arc related to plate subduction. In: Pharaoh, T.C., Beckinsale, R.D. and Rickard ,D. (eds.), Geochemistry and Mineralization of Proterozoic volcanic suites, Geol. Society Special Publication, 33: 437-448.

Druecker, M.D., 1985, Mafic dyke swarms associated with Mesozoic rifting in eastern Paraguay. Abstr. Int. Conf. Mafic dyke swarms, Univ. Toronto, Canada.

El Metwally, A.A., 1997, Sinai mafic and felsic dykes: Geochemistry and emplacement model. Egypt J. Geol. V. 41 (1), p. 357-386.

El Ramly, M.F. and Akaad, M.K., 1960, The basement complex in the Central Eastern Desert of Egypt between latitudes 24o 30` and 25o 40`. Geol. Surv. Egypt. Paper 8, 35pp.

Eyal, Y. and Eyal, M., 1987, Mafic dyke swarms in the Arabian-Nubian Shield. Isr. J. Earth Sci., V. 36, P. 1`95-211.

Feraud, G., Giannerini, G., Comperdon, R. and Mermet, J.F., 1985, Some examples of correlations between dyke swarms and geodynamic pattern in the Mediterranean area. Abstr. Int. Conf. Mafic dyke swarms, Univ. Toronto, Canada.

Friz-Töpfer, A., 1991, Geochemical characterization of Pan African dyke swarms in southern Sinai: from continental margin to intraplate magmatism. Precambrian Res., V. 49, P. 281-300.

Goldberg, S.A. and Buttler, J.R., 1985, The Bakerville dyke swarm: a record of Late Proterozoic rifting in the southern Appalachians. Abstr. Int. Conf Mafic Dyke swarms, Univ. Toronto, Canada.

Hooper, P.R. and Subbarao, K.V., 1985, Feeder dykes to the Columbia River and Deccan Basalts. Abstr. Int. Conf. Mafic Dyke swarms, Univ. Toronto, Canada.

Hutchinson, R.M., 1956, Structure and petrology Enchanted Rock Batholith, Llano and Gillespie Counties. Texas. Geol. Soc. Am. Bull. 67: 763-806.

Irvine, T.N. and Baragar, W.R.A., 1971, A Guide to the Chemical Composition of the Common Volcanic Rocks, Can. Jour. Earth Sci., 8, 523-548.

Katta, L.A.S., 1994, Geochemistry and tectonic environment of post-granite dykes north of Wadi Feiran area, South Sinai, Egypt. Mansoura Sci. Bull., V. 21 (2), P.267-289.

Krauskopf, K.B., 1979, Introduction to geochemistry. 2nd Ed. McGraw-Hill Book Co. London, 617p.

Le Bass, M.J., Le Maitre, R.W., Streckeisen, A. and Zanettin, B. (1986), A chemical classification of volcanic rocks based on the total alkali silica diagram. J. Petrol., 27, 3, 745-750.

Martin, N.R., 1952, The structure of the granite massif of Flamanville, Manche, North West France. J. Geol. Soc. London, 108: 311-341.

Miyashiro, A. (1975), Classification, characteristics and origin of ophiolites. J. Geol., 83, p. 249-281.

Mousa, H.E., 1994, Petrography and opaque mineralogy of rocks along Feiran-Catherina road, Central Sinai, Egypt. Mineral., V.6.P. 13-29.

Pagel, M., 1982, The mineralogy and geochemistry of uranium and thorium and rare earth elements in two radioactive granites of the Vosages, France, Mineralogical Magazine 46, pp. 152-173.

Pearce, J.A., 1983, The role of sub-continental lithosphere in magma at destructive plate margin. In Howkesworth, C.J. and Norry, H.J. (ed.) Continental basalt and mantle xenoliths, Natwich, Shiva: 230-294.

Pearce, J.A. and Cann, J.R., 1973, Tectonic setting of basic volcanic rocks determined using trace element analysis. Earth Planetary Science Letters 19, 290-300.

Pearce, J.A., Harris, N.B.W and Tindle, A.G., 1984, Trace element discrimination diagrams for the tectonic interpretation of granitic rocks. J.Petrol., 25(4):956-983.

Philips 1994. X40 Software for XRF analysis. Software Operation Manual. 425p. Nederlandse Philips Bedrijven, Amsterdam.

Rogers, J.J.W. and Adams, J.S.S., 1969, Uranium, in Wedepohl. K.H. (ed.) Handbook of geochemistry. New York, Springer-Verlag, vol.4, p. 92 B1-92 C10.

Ross, M.E., 1983, Chemical and mineralogical variations within four dykes of the Columbia River Basalt Group, southeastern Columbia Plateau. Geol. Soc. Am. Bull. V. 94, P. 1117- 1126.

Stern, R.J. and Hedge C.E., 1985, Geochronologic and isotopic constraints on Late Precambrian crustal evolution in the Eastern Desert of Egypt. Am. J. Sci., 285: 97- 127.

Stern, R.J., Gottfried, D. and Hedge, C.E., 1984, Late Precambrian rifting crustal evolution in the northeastern Desert of Egypt. Geology. 12: 168- 172.

Sun, S.S. and Nesbitt, R.W., 1978, Geochemical regularities and genetic significance of ophiolite basalts. Geology. 6: 689-693.

Tatsumi, Y., Hamilton, D.L. and Nesbitt, R.W., 1986, Chemical characteristics of fluid phase released from a subducted lithosphere and origin of arc magmas: evidence from high-pressure experiments and natural rocks. J.Volcan. Geoth. Res. 29: 293-309.

Wyllie, P. J., Corroll, M.R., Johnston, A.D., Rutter, M.J., Sekine, T. and Vanderlaan, S.R., 1989, Introduction among magmas and rocks in subduction zone regions: experimental studies from slab to mantle to crust. European Journal Mineralogist, 1: 165-179.

Zalata, A.A., 1988, On the dyke swarms of Wadi El-Akhdar area Centeral Sinai, Egypt. Mansoura Sci. Bull., V. 15 (2), P.245-269.

ALI ALI ABDEL RAHMAN EL MOWAFY

جيولوجية وكيميائية وأشعاعية الجدد بمنطقة جبل منادير - جنوب وسط سيناء- مصر

على على عبد الرحمن الموافى

هيئة المواد النووية- ص. ب. -٥٣٠ المعادى ،القاهرة ،مصر

تقع منطقة الدراسه بين خطى عرض ٣٢ ٤٠ً ٢٨ْ و ٤٠ ٤٥ً ٢٨ْ شمالا وخطى طول ١٢ً ٥٤ْ ٣٣ و ٤٨ً ٠٣ْ ٣٤ شرقا بجنوب وسط سيناء وتغطى مساحة ٩٠ كم٢ من صخور البريكمبرى. تركزت الدراسه على الجدد القاطعه لصخور البريكمبرى التى تغطى منطقة البحث ومن خلال الدراسة الجيولوجية والتركيبية أتضح أن هذه الجدد تداخلت فى ثلاث مراحل متعاقبه من تداخل الصهير فى صخور المنطقة. ألمرحلة ألاولى شملت جدد ألرايولايت وهى ألأكثر شيوعا فى منطقة البحث وتتجه إلى شمال شرق وأن هناك بعض الجدد من هذا النوع منحرفة قليلا إلى اتجاه شمال شمال شرق وشرق شمال شرق أما ألمرحلة ألثانيه فشملت جدد ألأنديزايت وألتى تتجه نحو شمال غرب. أما ألمرحلة ألثالثه وألأخيرة شملت جدد ألأنديزى بازلت والتى تتجه إلى شمال شمال غرب وشمال غرب وقليل إلى شمال شرق

وبدراسة نظم ألأجهاد ألقديم المسئول عن نشأة هذه ألأتجاهات التركيبيه أتضح أن ألأتجاهات التركيبيه لقواطع المرحله ألأولى ٥٠شرق بينما قواطع المرحلة الثانيه ترجع٥ فى أتجاه جنوب 650 ترجع إلى شد فى صخور ألقشرة ألأرضيه حيث σ٣ إلى شد ذات σ٣ =٨٠٥ فى أتجاه جنوب٥ ٦٠غرب وأخيرا ترجع قواطع المرحلة الثالثه إلى شد ذات σ٣=٦٠٥ فى أتجاه جنوب٥ ٣٨ غرب

وأوضحت الدراسه الجيوكيميائيه أن هذه الجدد قد نشأت من مجما كلس قلويه غنيه بأكسيد التيتانيوم وتكونت بالتبلور التجزئى ومنها جدد ألأنديزايت تبعها جدد الأنديزى بازلت وبزيادة تفارق المجما تكونت جدد الرايولايت ألأكثر تفارقا وأقل فى نسبة أكسيد التيتانيوم. وقد نشأت هذه الجدد فى اقواس الحمم البركانيه واواسط الهضاب البازلتيه المحيطيه. وقد تمت دراسه توزيع النشاط الأشعاعى للجدد المختلفه بمنطقة البحث وتبين أن لكل نوع من الجدد قيم إشعاعيه خاصه تميزه عن غيره من الجدد ولوحظ أن جدد الرايولايت القلوى ذات شذات أشعاعيه عاليه وبتحليل عينات من هذه الشاذات بأستخدام جهاز الماسح الألكترونى وجهاز حيود الأشعه السينيه تم التعرف على المعادن الحامله لليورانيوم وهى البيروكلور والبيتافايت والشوبايت والأوكزونايت واليورانوثورايت والزركون.